CA9900148

INVESTIGATION OF COOLANT THERMAL MIXING WITHIN 28-ELEMENT CANDU FUEL BUNDLES USING THE ASSERT-PV THERMAL HYDRAULICS CODE

M.F. LIGHTSTONE

Department of Mechanical
and Industrial Engineering
University of Toronto
5 King's College Road
Toronto, Ontario M5S 3G8

R. ROCK

Reactor Safety and
Operational Analysis Department
Ontario Hydro Nuclear
700 University Avenue
Toronto, Ontario M5G 1X6

Abstract

This paper presents the results of a study of the thermal mixing of single-phase coolant in 28-element CANDU fuel bundles under steady-state conditions. The study, which is based on simulations performed using the ASSERT-PV thermal hydraulic code, consists of two main parts. In the first part the various physical mechanisms that contribute to coolant mixing are identified and their impact is isolated via ASSERT-PV simulations. The second part is concerned with development of a preliminary model suitable for use in the fuel and fuel channel code FACTAR to predict the thermal mixing that occurs between flow annuli.

INTRODUCTION

The foundation of the Canadian nuclear electric industry is the successful CANDU reactor. Thorough and accurate assurance of the safety of the CANDU design is an essential component of the responsibility borne by the designers, owners, and operators of the reactor. One aspect of this safety assurance is met through detailed analysis of the behaviour of the fuel bundles and horizontal fuel channels during a postulated large break loss-of-coolant accident (LOCA).

In order to perform an analysis of the fuel and fuel channel performance during a LOCA, the Reactor Safety and Operational Analysis Department of Ontario Hydro Nuclear has developed the computer code FACTAR (Fuel And Channel Temperature And Response [1]). FACTAR is an advanced fuel channel simulation program combined with suitably accurate fuel element, thermal hydraulic and pressure tube/calandria tube models. Using channel inlet thermal hydraulic transients (i.e., coolant pressure, mass flow, and enthalpy) in conjunction with detailed pre-transient fuel pellet thermophysical characteristics and a channel power transient, FACTAR calculates transient thermal and mechanical response of the UO_2 fuel pellets and their Zircaloy sheath. In addition, detailed oxidation and high temperature Zircaloy behaviour models are used in the sheath thermal and mechanical calculations.

The bundle geometry used in CANDU reactors poses a challenge to engineers attempting to model flow within the bundle. Due to the complexities of the flow associated with this bundle geometry, highly detailed numerical simulation of the flow field is often impractical. Hence, FACTAR uses up to four flow annuli (as illustrated in Figure 1) to model coolant flow. These flow annuli, which correspond roughly to gaps between neighbouring concentric rings of fuel elements, represent control volumes over which coolant energy is conserved.

In FACTAR versions prior to 2.0, momentum and mass equations are not directly solved. Rather, it is assumed that along the fuel channel, pressure and mass flow rate are constant. The transient energy equation is solved assuming a fully advective, homogeneous mixture. These assumptions allow for an efficient, parabolic thermal hydraulic solution, which provides boundary conditions to the complex fuel and sheath models. As a result of this treatment, however, a detailed description of the velocity field is not calculated. Hence, thermal mixing and the redistribution of mass between flow annuli and between bundles must be specified empirically.

The distribution of coolant is currently calculated by assuming equal flow resistances at each flow annulus. Hence, for coolant at a uniform density, the flow distribution is determined directly from the area fractions at each flow annulus. The exchange of energy between radially adjacent flow annuli is modelled through

FACTAR's mixing treatments. These include: total mixing along a bundle; partial mixing along a bundle; total mixing at end plates; or partial mixing at end plates. These treatments are invoked by changing the number of coolant control volumes per bundle (i.e., 'total mixing along a bundle' combines all four flow annuli into a single control volume while 'partial mixing' does combines the enthalpy of the four flow annuli at the end plate) or by changing the method used to calculate the coolant enthalpy entering a flow annulus (i.e., 'total mixing at endplates' assumes that for a given bundle, the same enthalpy enters each flow annulus).

An important requirement of FACTAR's use in CANDU safety analysis and licensing is to evaluate the strengths and limitations of the code's mixing assumptions. One method for accomplishing this assessment is to analyze coolant behaviour using a code with a thermal hydraulics calculation more rigorous than FACTAR's. One such code is ASSERT-PV (Advanced Solution of Subchannel Equations in Reactor Thermalhydraulics, Pressure-Velocity [2]) developed at Atomic Energy of Canada, Ltd. under CANDU Owner's Group (COG) Working Pary 7 funding and direction.

ASSERT-PV models single- or two-phase flow through the bundle on a subchannel basis, as opposed to FACTAR's flow annulus approach. The term 'subchannel' refers to a small flow area within a bundle bounded by several fuel elements. The subchannels for one symmetrical half of a 28-element fuel bundle are shown in Figure 2. Fully three-dimensional, the code numerically solves the coupled conservation equations for mass, momentum, and energy for each phase using the subchannel grid. Relative velocities between the phases are estimated using a drift-flux correlation. ASSERT-PV does not, however, model the thermomechanical response of the fuel, sheath, or pressure tube; it is strictly a subchannel thermal hydraulic code.

The greater rigor of ASSERT-PV's thermal hydraulics models provides the investigator with increased flow solution detail. In addition, through the use of phenomenological models, the effects of the important physical phenomena on coolant behaviour can be carefully studied to gain an understanding of the underlying fluid mechanics. This allows for model development with a strong physical foundation. In this paper, the coolant mixing within a 28-element CANDU bundle is considered. This bundle geometry corresponds to that used in Ontario Hydro's Pickering nuclear generating stations.

In this paper, the physical mechanisms producing mixing are discussed, with emphasis on mixing due to buoyancy, turbulence, and obstructions. An analysis methodology is explained, through which the relative impacts of these mixing mechanisms are investigated. A preliminary mixing model is presented for application to the flow annuli used by FACTAR.

DISCUSSION OF PHYSICAL MECHANISMS PRODUCING MIXING

In order to understand the fluid flow behaviour both within a bundle and along the entire channel length, the various mechanisms which contribute to mixing of a single-phase liquid must be identified and their effects isolated. Factors which contribute to coolant mixing have been identified as: buoyancy (i.e., gravitational forces), fluid turbulence, and obstructions in the channel (i.e., spacers and endplates). These mixing mechanisms and their modelling treatment in ASSERT-PV are discussed below.

Buoyancy: As a result of geometric eccentricities in the placement of the fuel bundle in the pressure tube, subchannels adjacent to the bottom of the pressure tube are smaller than those near the top. This geometry results in higher local coolant temperatures near the bottom of the pressure tube due to reduced mass flow in this region. This unstable stratification (due to lower density fluid situated below higher density fluid) promotes mixing of the coolant through natural convection forces. ASSERT-PV models buoyancy through inclusion of the gravitational term in the momentum equations. The inclusion of the gravitational force is a user-specified option.

Turbulence: Turbulence aids mixing in the channel by enhancing convective transport of momentum and energy across flow annuli. The effect of turbulence is modelled empirically in ASSERT-PV using a turbulent diffusion approach. It should be noted that while this type of turbulence model is available for the vapour phase very little information is available on the appropriate specification of the required model constants. Due to this uncertainty, the default calculation mode of ASSERT-PV for coolant in the vapour phase does not allow for turbulent transport of energy. In contrast, turbulent transport is modelled for liquid coolant

due to a more substantial data base upon which to determine model constants. Turbulence modelling. in general, represents a challenging area of computational fluid dynamics and the use of very simple models should be viewed with caution.

Obstructions: Obstructions promote coolant mixing in the fuel channel by distorting the pressure field such that fluid is diverted away from the obstructed area thus producing cross-flow mixing. Obstructions also act to enhance fluid turbulence by creating large velocity gradients. ASSERT-PV models obstructions in the channel by applying local (i.e., on a subchannel basis) loss coefficients (K-factors) at the location of the obstruction. Two approaches can be used to model obstructions. The first treats the losses due to spacers and endplates as being uniformly distributed (i.e., smeared) across the bundle cross-section. The second approach models the losses in a non-uniform manner. The latter approach, which allows for differential blocking of the various subchannels, is more representative of the actual endplate and spacer geometries.

Analysis Methodology

The approach adopted in this work is to examine the impact of the various mixing mechanisms by performing ASSERT-PV simulations with each mechanism considered independently. This allows for individual mixing mechanisms to be understood. The first step, therefore, was to establish a reference solution where none of the mixing mechanisms are modelled. Hence, simulations were performed for a channel with no obstructions, and with buoyancy and turbulence effects neglected. For a fully developed flow (i.e., one in which the mass flow in individual flow annuli does not change with axial location) under such conditions, there is no mechanism to transport energy between flow annuli, hence the coolant characteristics in each annulus are independent from the coolant characteristics in the neighbouring flow annuli. This condition is referred to in this work as a 'zero-mixing' condition.

Simulations were then performed with each of the mixing mechanisms considered independently. Comparison of predictions to the 'zero-mixing' results allow for the impact of the individual mechanisms to be understood. Finally, coupling of the effects was studied through simulations with the effects considered simultaneously.

The following models were therefore considered:

1. 'Zero-Mixing' (turbulence, buoyancy, and obstructions not modelled)
2. Turbulence only (available for simulations with liquid coolant only)
3. Gravity/Buoyancy only
4. Obstructions only
   4a) Uniform K-Factors
   4b) Non-Uniform K-Factors
5. 'Coupled Effects' (turbulence, buoyancy, and non-uniform obstructions together)

The impact of the mixing mechanisms described above was studied for the operating conditions given in Table 1. The Reynolds numbers provided in Table 1 are based on the channel hydraulic diameter and the average channel velocity. The range in the Reynolds number for a given case is a result of the changes to the dynamic viscosity, μ, due to the temperature increase of the coolant as it flows along the channel. Low flow rates of steam (50 g/s and 250 g/s) were chosen because such flow rates are relevant to large break LOCA conditions. Because of the difficulties of modelling the thermal mixing due to turbulence for the vapour phase, liquid flows with similar Reynolds numbers were also considered. The fuel powers were chosen to give the same enthalpy increases along the channel for each of the phases. Low inlet enthalpies for the liquid simulations were used to ensure that there was no local boiling. Because the heat transfer to the pressure tube from the coolant in the outer flow annulus was not accounted for directly in the ASSERT-PV simulations, a radial flux distribution which provided a reduced heat flux to the outer annulus was implemented. All simulations were performed at an outlet pressure of 4 MPa. Only steady state conditions were considered, using nominal 28-element bundle geometries. All simulations were performed on Ontario Hydro's IBM RS-6000 series of computers using ASSERT-PV Version 2.7. A grid allowing for five axial nodes per bundle was employed.

Analysis Results

ASSERT-PV simulations provide detailed descriptions of the fluid flow and heat transfer at each subchannel along the channel. For the purpose of this work, however, the interest is in the mixing that occurs on a

broader scale: i.e., between flow annuli rather than between subchannels. Hence, ASSERT-PV output is post-processed here by integrating the ASSERT-PV predictions over the subchannels contained in each flow annulus. The subchannel layout for a 28-element bundle is shown in Figure 2 and the subchannels comprising each flow annulus is given in Table 2.

The average enthalpy for a flow annulus at axial location x is calculated from:

$$\overline{h_i}(x) = \frac{\sum_{j=JB}^{j=JE} h_j(x)\dot{m}_j(x)}{\sum_{j=JB}^{j=JE} \dot{m}_j(x)} \tag{1}$$

where $\overline{h_i}(x)$ is the integrated enthalpy for flow annulus i (kJ/kg), $h_j(x)$ is the coolant enthalpy at subchannel j (kJ/kg), $\dot{m}_j$ is the mass flow through subchannel j (kg/s), and JB and JE are the range of subchannels comprising flow annulus i.

The mass flow in an annulus at a given axial node is calculated as the sum of the mass flows in each subchannel contained in that flow annulus:

$$\dot{m}_i(x) = \sum_{j=JB}^{j=JE} \dot{m}_j(x) \tag{2}$$

Zero-Mixing Simulations

As discussed earlier the zero-mixing simulations provide a benchmark against which each of the individual mixing mechanisms are measured. For a flow with no mixing between flow annuli, the enthalpy increase along a bundle can be calculated analytically from knowledge of the mass flow through the flow annulus and the fuel power added to the coolant:

$$\Delta h_i(x) = \frac{Q_{\text{fuel}}}{\dot{m}_i} \tag{3}$$

To determine how close an ASSERT-PV simulation is to a true zero-mixing situation, ASSERT-PV results are compared to those calculated analytically assuming no communication between flow annuli. The mass flow used in Equation (3) is the value calculated by ASSERT-PV at the centre of bundle 7 for flow annulus i. Bundle 7 is chosen as it is near the centre of the channel and therefore is furthest from the channel boundary conditions.

Figure 3 shows the enthalpy increase per bundle along the channel for case AL. The curves represent integrated ASSERT-PV predictions. The symbols are calculations of enthalpy increases (Equation (3)). Excellent agreement between ASSERT-PV predictions and calculated enthalpy increases (based on ASSERT-PV mass flows) are seen. This result confirms that removing buoyancy, turbulence, and obstructions produces a situation where coolant flows along the channel undisturbed. Hence, confidence in the identified mixing mechanisms is obtained.

The net axial convective energy transport and the fuel energy input are shown in Figure 4. The curves represent the axial convective terms and the symbols represent the energy from the fuel added to the coolant. The imbalance at the start of the channel indicates the development region of the flow (Figure 5). Further downstream, the net axial convection almost balances the heat addition from the fuel.

Although not presented here, the conclusions drawn for cases BL and BV were similar to that described above. A converged ASSERT-PV solution was not obtained for case AV (vapour at 0.050 kg/s). The lack of convergence is attributed to the non-physical imposed conditions: very low flows and high temperatures that appear in the small subchannels from the imposition of the zero-mixing constraint.

Gravity/Buoyancy Effects

Figure 6 shows the predicted enthalpy increases per bundle for flow annuli when gravitational effects are included. Results are shown for case AL only. The enhanced mixing resulting from the buoyancy forces reduces the differences between the curves relative to the no-mixing case. Indeed, for a fully mixed flow the

enthalpy increase at each flow annulus would be the same and the four curves shown on the figures would collapse onto a single curve. A qualitative measure of the degree of mixing can be found by considering the predicted enthalpy increase relative to that for a fully mixed flow:

$$\text{Separation Parameter} = \sqrt{\frac{\sum_{i=1}^{i=4}(\Delta h_i(j) - \Delta h_{FM}(j))^2}{4}} \tag{4}$$

where $\Delta h_i(j)$ is the enthalpy increase for flow annulus i at bundle j (calculated from ASSERT-PV results) and $\Delta h_{FM}(j)$ is the enthalpy increase at bundle j for fully mixed flow (calculated analytically).

The parameter defined by Equation (4) represents, roughly, the standard deviation of the enthalpy increase from the fully mixed value. Thus, a value of zero indicates a fully mixed flow if the same enthalpy enters each flow annulus of a given bundle.

Figure 7 shows the values of Equation (4) for the liquid (Cases AL and BL) simulations. Also shown on the figure, for reference, are the values of the parameters obtained for the zero-mixing case. The zero-mixing case values on Figure 7 indicate the maximum values of the separation parameter. The greater the departure from the zero-mixing value, the more pronounced is the mixing. From the two figures, it is seen that mixing due to buoyancy is enhanced with decreasing Reynolds number. This result is consistent with a scaling of the buoyancy term in the momentum equation: as inertia increases, the driving force due to buoyancy is diminished. Similar conclusions were drawn for the vapour simulations (Cases AV and BV).

Turbulent Thermal Mixing

The separation parameters for simulations with turbulent thermal mixing included are shown in Figure 8. As discussed earlier, simulations with turbulent thermal mixing were not performed for the superheated steam cases because of the uncertainty in the turbulent model constants. It is seen that turbulence plays a strong role in mixing the coolant, with the degree of mixing being relatively insensitive to the Reynolds number, for the range of conditions investigated.

Flow Obstructions

Uniform K-Factors: In this set of simulations, the effects of the endplates and spacers on fluid pressure drop and flow were modelled by applying uniform K-factors across the bundle at the axial locations corresponding to the placement of the bundle appendages. With uniform K-factors applied, the flow is redistributed away from the larger subchannels since the coolant flows at a higher velocity in these subchannels and experiences a higher loss at the appendage location. ASSERT-PV results show that as an appendage is approached, the flow is diverted towards the innermost and outermost flow annuli. These changes in the flow are fairly small, however, representing about 2% of the flow through the annulus. Hence, with uniform K-factors applied, the impact on the mixing is fairly minor. This result is clearly demonstrated in Figure 9 through the large values of the separation parameter. Similar conclusions were reached for the vapour simulations.

Non-Uniform K-Factors: A more realistic assessment of the impact of spacers and endplates on coolant mixing was obtained by performing ASSERT-PV simulations using non-uniform K-factors at the bundle appendages. The geometry at the endplates is such that a partial blockage is applied to the larger subchannels (#2, 4, and 6 in Figure 2) in flow annulus 2 as well as to the small subchannels in flow annulus 3 (#8, 10, 12, and 14). As seen in Figure 10, as an endplate is approached there is a sharp drop in the mass flow in flow annulus 2 and a corresponding increase in the flow through flow annulus 4. This strong flow redistribution results in enhanced mixing of the coolant. Figure 11 shows the separation parameter for the liquid simulation. These low values relative to the zero-mixing case indicate the increased mixing due to the appendages. Further, a Reynolds number dependence is seen with more significant mixing occurring as the Reynolds number increases.

Simultaneous Modelling of Gravity, Turbulence, and Non-Uniform K-Factors at Bundle Appendages

The coupled effects of the various mixing mechanisms were assessed by performing simulations with turbulent thermal mixing, gravity, and non-uniform K-factors modelled simultaneously. Non-uniform K-factors were used since they model the non-uniformities of the end-plates and spacers more realistically than uniform

K-factors. Since, as discussed earlier, turbulent mixing cannot be modelled with confidence for the vapour phase, the simulations are restricted to single phase liquid. The enthalpy increase per bundle is shown in Figure 12 for case AL. The predicted enthalpy increases for the various flow annuli nearly collapse to a single line, indicating that the flow is very close to fully mixed. Figure 13 shows the separation parameter for the two cases. Again, the large departure from the zero-mixing case demonstrates the strong mixing that is present.

Summary of the Impact of the Mixing Mechanisms

The impact of the various mechanisms on mixing can be quantified for the flows considered through the following mixing parameter:

$$\text{MIXP} = 1.0 - \left\{ \frac{\text{Separation Parameter}}{\text{Separation Parameter for No Mixing}} \right\} \tag{5}$$

where the separation parameter is as defined in Equation (4). Note that the quantity 'MIXP' has the following limits:

MIXP = 0 - no mixing between flow annuli occurs
MIXP = 1 - the flow is fully mixed.

Values of Equation (5) at bundle 7 for all simulations performed are given in Table 3. Also shown in Table 3 are results from a case designated AAL. This was a supplementary (single phase liquid) simulation performed at a low mass flow of 0.25 kg/s and an energy input of 0.0496 MW. The Reynolds number range was from 900 to 2300. This run was performed to substantiate the Reynolds number trends that were seen. Unfortunately, a solution could not be obtained when gravity was included, so an assessment could not be made for the case where the effects are considered simultaneously.

From the cases considered, the following trends are noted:

i. turbulence has a strong impact on the mixing and is relatively insensitive to the Reynolds number;
ii. gravity is also an important factor in thermal mixing, but its influence is a function of the Reynolds number: as the Reynolds number increases, mixing due to gravity decreases; and
iii. non-uniform K-factors also enhance mixing as a function of Reynolds number, but with the opposite trend: as Reynolds number increases, the mixing due to appendages (modelled with non-uniform K-factors) increases. When the losses due to appendages are modelled with uniform K-factors, the mixing is insensitive to the Reynolds number.

When all the factors were considered simultaneously (this was possible for cases AL and BL only), the coolant was very close to fully mixed. A Reynolds number dependence was not seen, possibly due to the balancing effects of buoyancy and obstructions, which have opposite Reynolds number trends. Further simulations over a wider range of Reynolds number are required to substantiate this.

PRELIMINARY MODEL DEVELOPMENT

This section presents a methodology for model development to predict the coolant enthalpy in a flow annulus with communication between neighbouring flow annuli accounted for. The development is founded on a steady state energy balance for the coolant in a flow annulus (see Figure 14):

$$\dot{m}_e h_e = \dot{m}_w h_w - (Q_{T,n} - Q_{T,s}) + Q_{Fuel,i} \tag{6}$$

where:

$\dot{m}_w$ = axial mass flow entering the flow annulus (kg/s),
$\dot{m}_e$ = axial mass flow leaving the flow annulus (kg/s),
h_w = enthalpy of coolant entering the flow annulus (kJ/kg),
h_e = enthalpy of coolant leaving the flow annulus (kJ/kg),
$Q_{T,n}$ = energy transfer from the north side of annulus (kW),
$Q_{T,s}$ = energy transfer entering the south side of annulus (kW), and
$Q_{Fuel,i}$ = fuel energy added to annulus (kW).

The term $(Q_{T,n} - Q_{T,s})$ is the net transverse (radial) energy transport across the flow annulus. This term dictates the thermal mixing in the bundle.

In order to accurately predict the coolant enthalpy exiting a flow annulus, all the dominant terms in the energy equation need to be well predicted. Hence, good estimates of the mass flow through each annulus are required. While this preliminary model development has not been concerned with modelling the mass flow rates, it is recommended that ASSERT-PV predictions be used to determine an effective hydraulic diameter for each flow annulus. This methodology would allow for standard correlations to be used to determine the flow fractions per annulus. The focus of the current work is on the estimation of the transverse transport terms in the energy balance equation.

It is proposed that the transverse transport for flow annulus i be calculated as a fraction of the fuel power transferred to flow annulus i:

$$\Delta Q_{T,i} = (Q_{T,n} - Q_{T,s})_i = \alpha_i Q_{Fuel,i} \tag{7}$$

where α_i indicates the magnitude of the transverse transport relative to the fuel power for flow annulus i. The coefficient α may be a function of the Reynolds number and other relevant dimensionless groups such as the Grashof number. Note that a positive value for the coefficient indicates that there is more energy leaving the flow annulus than entering in the transverse direction. A negative values implies that there is a net contribution to the energy in the flow annulus from transverse energy transport.

In order to obtain values for the transverse energy transport coefficients, α_i, a series of ASSERT-PV simulations were performed over a range of mass flows and fuel powers. Since the coefficient relates the net transverse energy transport to the energy input to the flow annulus from the fuel, a sensitivity to the assumed radial flux distribution is expected. Therefore, for the ASSERT-PV simulations performed to determine the coefficients, a radial flux distribution that is typical of CANDU fuel was imposed and is given in Table 4.

Nine simulations were performed using three different mass flows and three different powers for each flow; the flow rates and fuel powers chosen range over one order of magnitude. The mass flows and fuel powers used are given in Table 5. All simulations were performed at an outlet pressure of 4.0 MPa and inlet enthalpy of 82.9 kJ/kg. Only single phase liquid was considered.

Figure 15 shows the calculated transverse transport coefficients for each flow annulus and at each bundle for case M1Q1. The large changes in the coefficients near the channel entrance reflect the flow development that is occurring in that region. The behaviour near the channel outlet is likely due to the outlet boundary conditions. Similar behaviour was seen for the other eight cases.

The predicted coefficients for bundle 7 for all nine cases are plotted as a function of Reynolds number in Figure 16. With the Reynolds number plotted on a log-scale, the data are seen to collapse to single lines for each flow annulus. From the figure the following trends are observed for the limited number of cases studied:

i. the transport coefficient for flow annulus 1 is positive and shows little variation with Reynolds number. A positive value for the coefficient implies that the energy transport is from flow annulus 1 to flow annulus 2, since there is no net transport across the bundle center;
ii. for flow annulus 2, the coefficient clearly increases with increasing Reynolds number from a negative value at low Reynolds numbers to a positive value at higher Reynolds numbers. The negative value for low Reynolds numbers implies that there is a net addition of heat to the flow annulus from its neighbours, while at the higher Reynolds numbers, the coolant in that flow annulus experiences a net loss of heat in the transverse direction;
iii. the net transverse transport for flow annulus 3 is large (relative to that seen for the inner two flow annuli) and is positive for all the Reynolds numbers considered; and
iv. for flow annulus 4, the coefficient is also large in magnitude but is negative and decreases with increasing Reynolds numbers. Hence, flow annulus 4 is gaining energy through transverse transport of energy from flow annulus 3 and the net gain increases with Reynolds number.

In general, the most important transverse transport is between flow annulus 3 and flow annulus 4. There is also a trend, for cases with the same total mass flow, for the magnitude of the coefficients for flow annuli 3 and 4 to increase with increasing power. This enhanced mixing is expected since buoyancy forces will be stronger at higher powers.

SUMMARY

This work was concerned with understanding the physical mechanisms that contribute to thermal mixing of coolant in 28-element fuel bundles as the coolant flows along the channel, and with developing a preliminary model to predict the coolant mixing that is consistent with the flow annulus geometry in FACTAR. The physical mechanisms which impact strongly upon coolant mixing are turbulence, buoyancy, and cross-flow mixing due to obstructions. A systematic investigation was performed in which the impact of these mechanisms, both individually and in combination was assessed. When all mechanisms are incorporated simultaneously, very good mixing along the channel is observed.

Model development was performed to quantify and characterise coolant mixing over a range of mass flows and fuel element powers. The basis for the model was to derive a function which describes the transverse transport of energy between flow annuli. The results of ASSERT-PV simulations showed a collapse of the model coefficients to a Reynolds number functional form.

ACKNOWLEDGEMENTS

The authors wish to thank Mr. T. Balint of Ontario Hydro for his contributions in the initial stages of the work. The on-going support from Dr. J. Kiteley, Dr. M. Carver, and Ms. S. Junop of Atomic Energy of Canada Limited is also acknowledged with gratitude.

REFERENCES

1. WESTBYE, C., BRITO, A., MACKINNON, J., SILLS, H., and LANGMAN, V., "Development, Verification and Validation of the Fuel Channel Behaviour Computer Code FACTAR", presented at the 35th annual CNA/CNS conference, Saskatoon, Saskatchewan, June 4-7, 1995.
2. CARVER, M., KITELY, J., TAHIR, A., BANAS, A., and ROWE, D., "Simulation of Flow and Phase Distribution in Vertical and Horizontal Bundles Using the ASSERT Subchannel Code", Nuclear Engineering and Design, Vol. 122, pp. 413-424 1990.
3. MODTURC_CLAS User Documentation, Version 2.3.1, Advanced Scientific Computing, 1994.

Case #	Mass Flow [kg/s]	Power [MW]	Coolant Phase	Reynolds Number
AV	0.05	0.05	vapour	11700 to 5800
BV	0.25	0.25	vapour	58000 to 29000
AL	1.26	0.25	liquid	4800 to 12600
BL	6.70	1.33	liquid	25500 to 62000

Table 1: Operating conditions used for study of mixing mechanisms.

Flow annulus	ASSERT-PV subchannels
1 (inner)	1
2	2 to 6
3	7 to 15
4 (outer)	16 to 24

Table 2: ASSERT-PV subchannels comprising FACTAR flow annuli.

Case	Zero Mixing	Turb Mixing	Gravity only	Unif. K-Factors	Non-Unif K-Factors	All	Reynolds # Range
AAL	0	0.70	-	0.15	0.15	-	900 to 2300
AL	0	0.77	0.70	0.17	0.63	0.93	4800 to 12600
BL	0	0.74	0.57	0.13	0.75	0.92	25500 to 62000
AV	0	-	0.77	0.14	0.48	-	11700 to 5800
BV	0	-	0.46	0.13	0.69	-	58000 to 29000

Table 3: Predicted values of the mixing parameter defined in Equation (5).

Fuel Ring	# Elements	Relative Power
1	4	0.788
2	8	0.884
3	16	1.111

Table 4: Radial flux distribution used for preliminary model development.

Case	Mass Flow [kg/s]	Fuel Power [MW]
M1Q1	1.26	0.062
M1Q2	1.26	0.125
M1Q3	1.26	0.250
M2Q1	6.70	0.125
M2Q2	6.70	0.250
M2Q3	6.70	1.330
M3Q1	13.40	0.250
M3Q2	13.40	1.330
M3Q3	13.40	2.660

Table 5: Conditions used for preliminary model development.

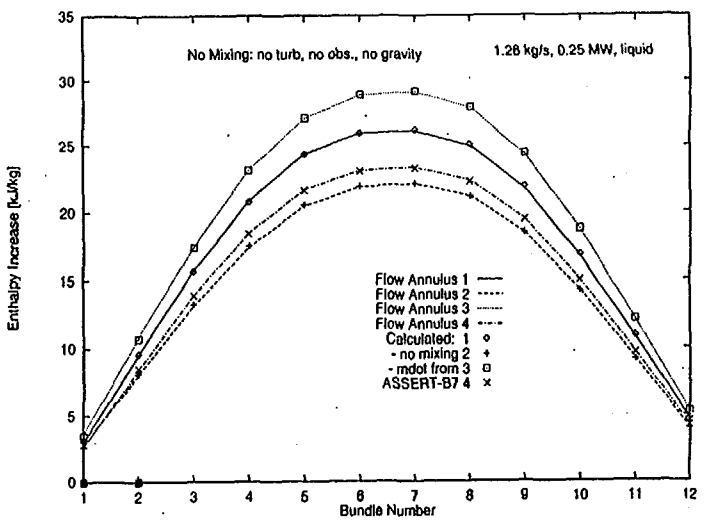

Figure 3: Enthalpy increase per bundle for a no-mixing condition.

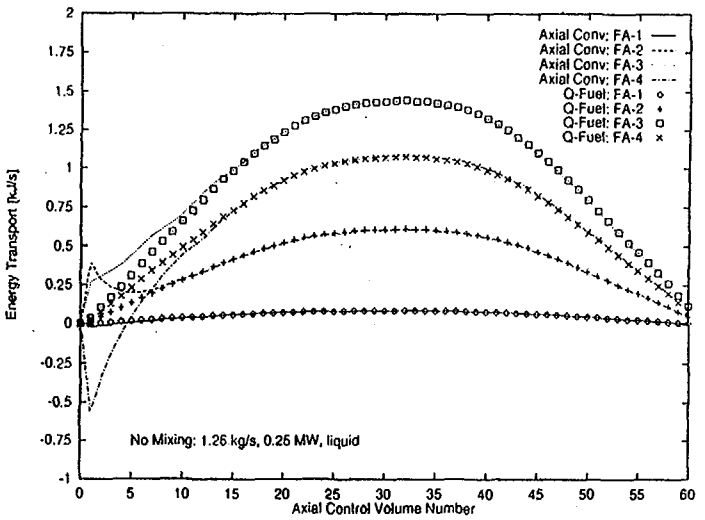

Figure 4: Net axial convective energy transport at each flow annulus.

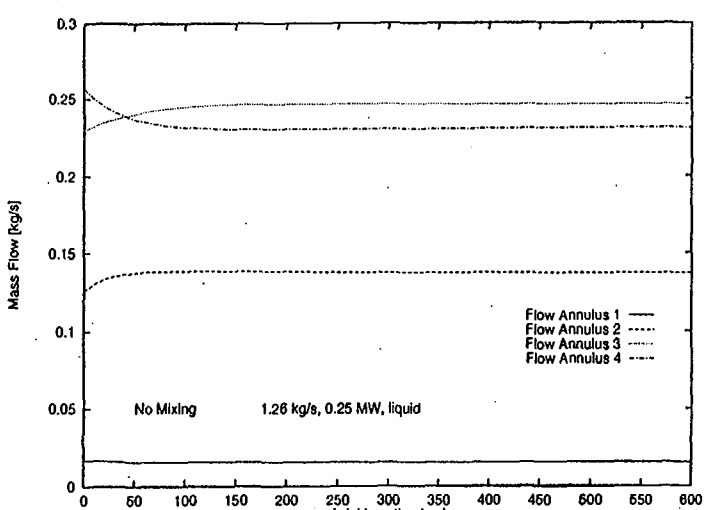

Figure 5: Mass flows at each flow annulus for Case AL with zero-mixing conditions (for half-bundle simulation).

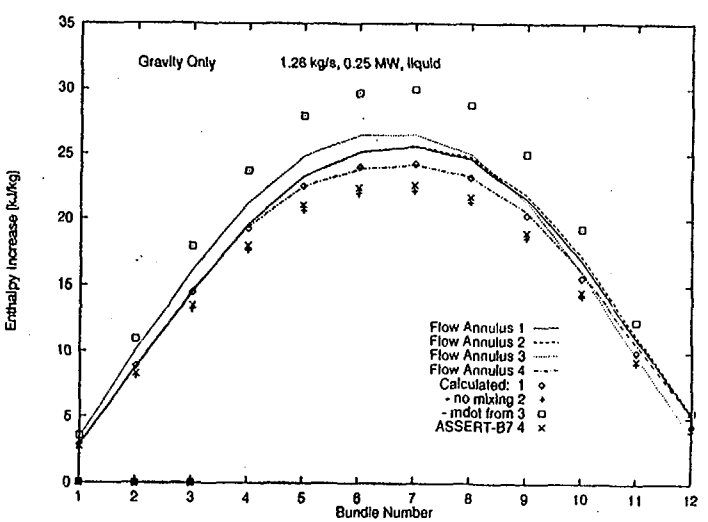

Figure 6: Enthalpy increases for Case AL with gravity only.

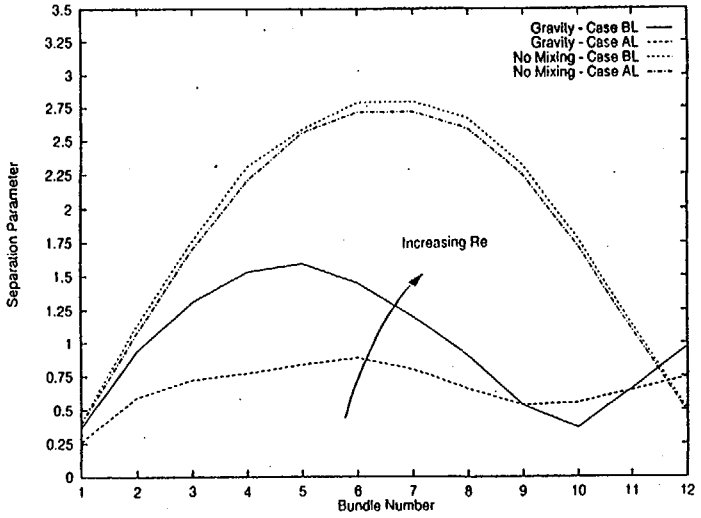

Figure 7: 'Separation Parameter' for Cases AL and BL with gravity only.

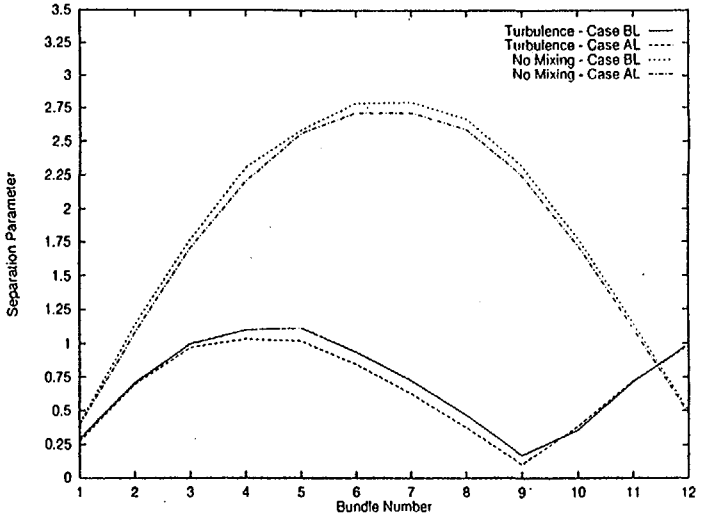

Figure 8: 'Separation Parameter' for Cases AL and BL with turbulence only.

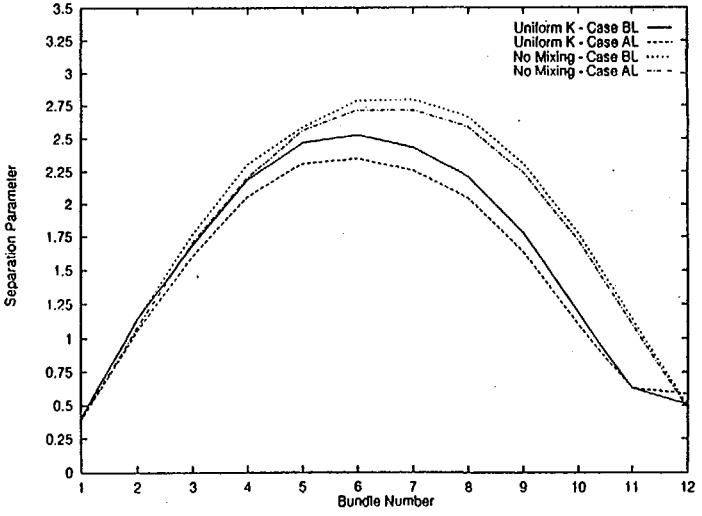

Figure 9: 'Separation Parameter' for Cases AL and BL with uniform K-factors.

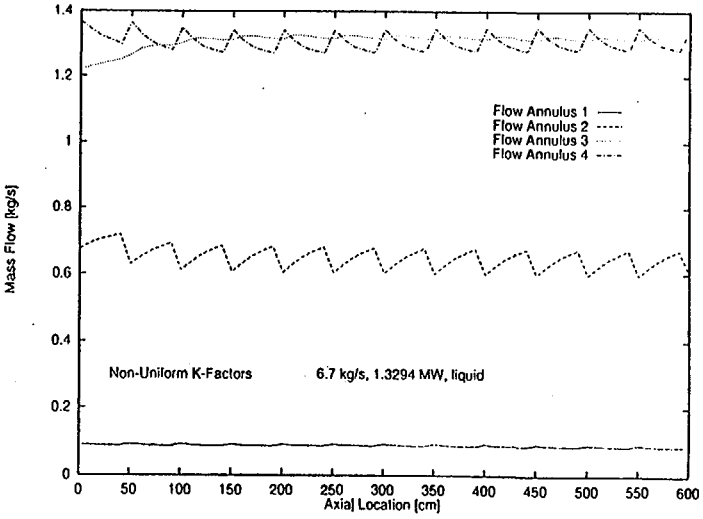

Figure 10: Mass Flows for Case AL with non-uniform K-factors (for half-bundle simulation).

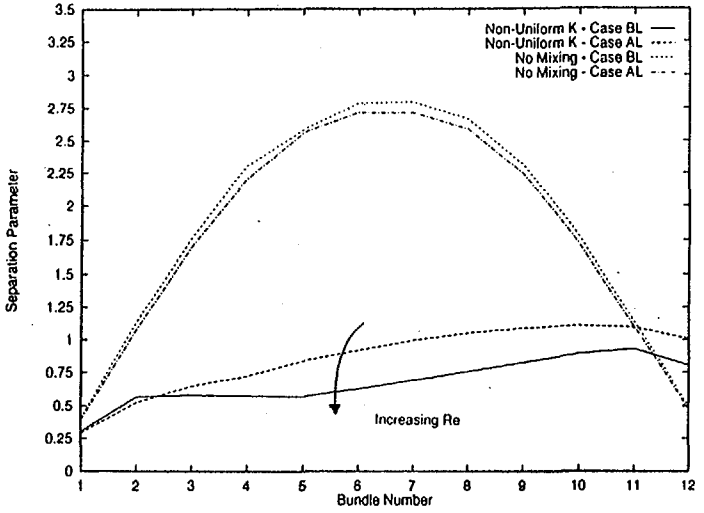

Figure 11: 'Separation Parameter' for Cases AL and BL with non-uniform K-factors.

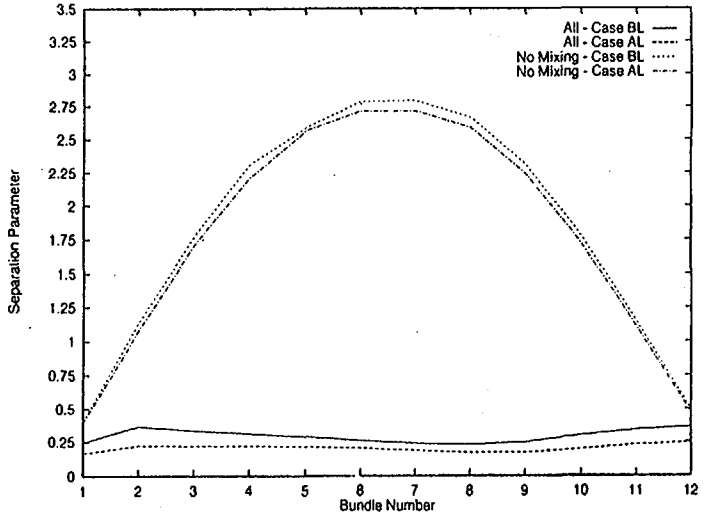

Figure 13: 'Separation parameter' for case AL with gravity, turbulence, and non-uniform K-factors modelled simultaneously.

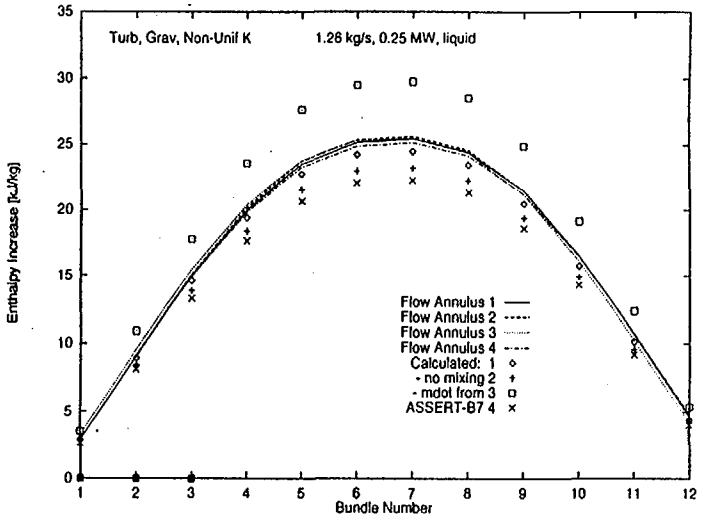

Figure 12: Enthalpy increases for case AL with gravity, turbulence, and non-uniform K-factors modelled simultaneously.

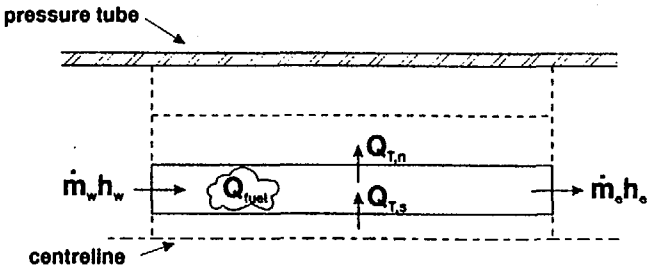

Figure 14: Energy transport at a flow annulus.

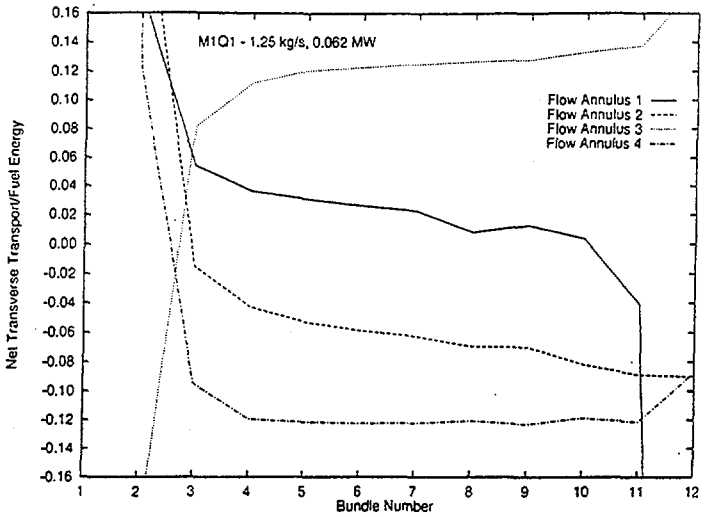

Figure 15: Ratio of net transverse energy transport to fuel energy for case M1Q1 with gravity, turbulence, and non-uniform K-factors modelled simultaneously.

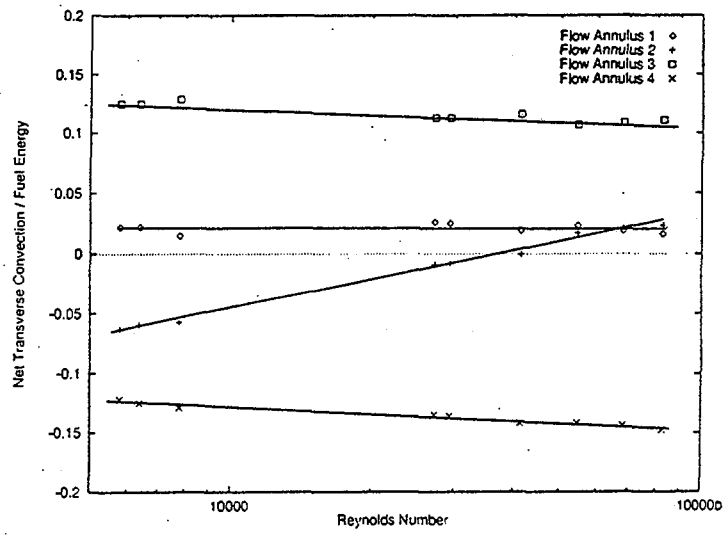

Figure 16: Ratio of net transverse energy transport to fuel energy as a function of Reynolds number.